Available online at www.sciencedirect.com
ScienceDirect
Journal of Molecular Spectroscopy 248 (2008) 122–133
Journal of MOLECULAR SPECTROSCOPY
www.elsevier.com/locate/jms

Intracavity laser absorption spectroscopy of HDO between 12 145 and 13 160 cm^{-1}

O.V. Naumenko [a], B.A. Voronin [a], F. Mazzotti [b], J. Tennyson [c], A. Campargue [b,*]

[a] *Institute of Atmospheric Optics, Russian Academy of Sciences, Siberian Branch, Akademicheskii av.1, Tomsk 634055, Russia*
[b] *Laboratoire de Spectrométrie Physique (associated with CNRS, UMR 5588), Université Joseph Fourier de Grenoble, B.P. 87, 38402 Saint-Martin-d'Hères Cedex, France*
[c] *University College London, London WC1E 6BT, UK*

Received 21 November 2007
Available online 23 December 2007

Abstract

The high resolution absorption spectrum of monodeuterated water, HDO, has been recorded by Intracavity Laser Absorption Spectroscopy (ICLAS) in the 12 145–13 160 cm^{-1} region. The achieved sensitivity (noise equivalent absorption on the order of $\alpha_{min} \sim 10^{-9}$ cm^{-1}) allowed detecting transitions with line strengths as weak as 10^{-27} cm/molecule which is about 50 times lower than the weakest line intensities previously detected in the considered region.

The rovibrational assignment of the 1179 lines attributed to the HDO isotopologue was based on the results of the variational calculations of Schwenke and Partridge as well as the recent calculations based on a new HDO potential energy surface refined from the fitting to the available experimental data. The overall agreement between these new calculations and the observed spectrum is very good, the *rms* deviation of the differences between the calculated and observed energy values being 0.05 cm^{-1}. A set of 304 new experimental HDO energy levels was obtained. In particular, band origins for the (1 2 2), (2 0 2), and (3 1 1) vibrational states, at 12 568.190, 12 644.652, and 12 919.938 cm^{-1}, respectively, and their rotational sublevels are derived for the first time. A detailed HDO database of 1337 transitions was constructed and is provided as Supplementary Material.

Keywords: Water; Monodeuterated water; HDO; Rovibrational spectroscopy; Intracavity Laser Absorption Spectroscopy (ICLAS)

1. Introduction

This work is part of our study of the absorption spectrum of HDO by Intracavity Laser Absorption Spectroscopy (ICLAS) with a Ti: Sapphire laser. In a first report, we analyzed the 11 645–12 330 cm^{-1} region dominated by the $v_2 + 3v_3$ band at 11 969.76 cm^{-1} [1]. The presently investigated 12 145–13 160 cm^{-1} region corresponds to weaker bands and extends to high energy our previous study. An overview of the spectrum as predicted by Schwenke and Partridge (SP) [4,5] in the 11 650–13 600 cm^{-1} region is presented in Fig. 1. Previous experimental investigations of HDO up to the visible region have been reviewed in Refs. [1–3]. The wide 11 500–23 000 cm^{-1} region has been recently studied by Fourier Transform Spectroscopy (FTS) associated with a 600 m path length [3,6]. Absolute line intensities and pressure shifts were obtained but in our region of interest, the sensitivity was not optimum (the detectivity threshold was about 5×10^{-26} cm/molecule for pure HDO). Another FTS spectrum, previously obtained in the 10 110–12 215 cm^{-1} with a 105 m absorption path length [8], has a similar sensitivity to that of Refs. [3,6]. This spectrum [8] does not show transitions in our region except the strongest lines in the narrow 12 145–12 214 cm^{-1} spectral section. The region of the $\Delta v_{OD} = 5v_1$ stretching overtone corresponding to the $5v_1$ band centered at 12 767.13 cm^{-1}, was also investigated by ICLAS associated with a FTS detection scheme [9]. Two

* Corresponding author. Fax: +33 4 76 63 54 95.
E-mail address: Alain.Campargue@ujf-grenoble.fr (A. Campargue).

0022-2852/$ - see front matter © 2007 Elsevier Inc. All rights reserved.
doi:10.1016/j.jms.2007.12.005

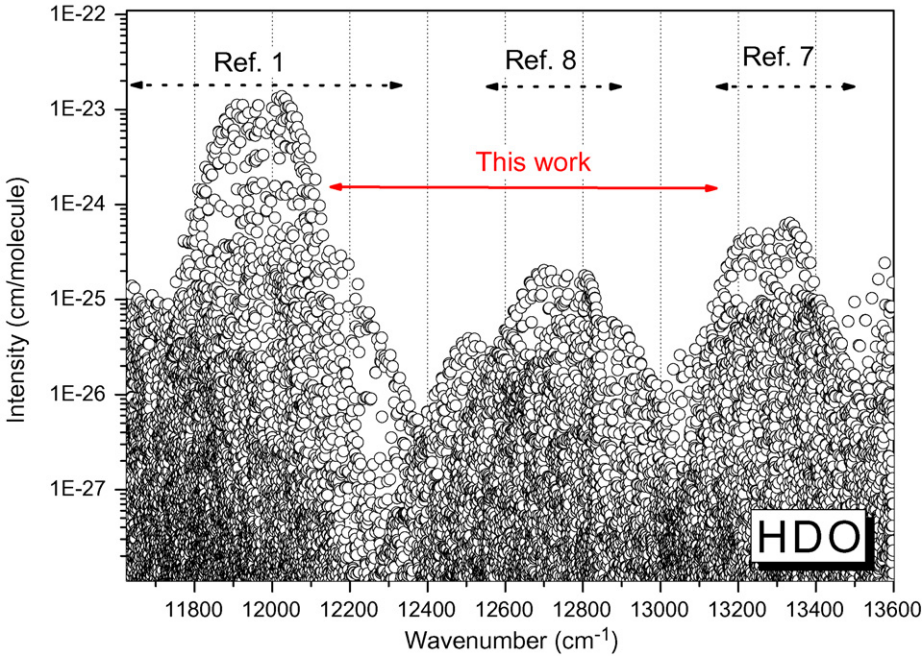

Fig. 1. Overview of the HDO spectrum in the 11650–13600 cm^{-1} region as predicted by Schwenke and Partridge [4,5]. The spectral regions previously investigated by ICLAS are indicated.

hundred and seventy-five lines were assigned in the 12550–12900 cm^{-1} region but the sensitivity was again similar to that of the recent FTS study [6]. For completeness, we mention the detection and assignment of about 120 transitions of the same $5v_1$ band in the 12720–12911 cm^{-1} by photoacoustic spectroscopy [10]. Compared to these four above studies, our increased sensitivity allows lowering the detection limit by at least a factor of 50, resulting in the detection of many new lines with intensities down to 10^{-27} cm/molecule. Finally, our investigation of the 13165–13500 cm^{-1} region by ICLAS with a dye laser [7] should be mentioned as some of the reported energy levels are upper levels of transitions lying in the presently investigated region.

2. Experimental details

The spectra were recorded with the ICLAS spectrometer based on a Ti: Sapphire laser as described in Refs. [1,11–13]. The only significant change is that a new intracavity absorption cell was designed and inserted in the Ti:Sa laser cavity in order to increase its occupation ratio. The length of the new cell is 65 cm which allowed increasing the filling ratio from 32% to 42%. The spectra were recorded with a generation time of 190 μs corresponding to an equivalent absorption path length of about 24 km. The intracavity sample cell was filled with a 1:1 mixture of H_2O and D_2O at a typical pressure of 18.4 hPa. A H_2O:HDO:D_2O mixture in a proportion of about 1:2:1 was then obtained. The spectral resolution fixed by the grating spectrograph was close to the Doppler line broadening. The 12145–13160 cm^{-1} region was covered by a total of 105 spectral snapshots overlapping by about 4 cm^{-1} on each side. Additional recordings were performed at lower pressures in the spectral regions corresponding to the stronger transitions, so as to obtain well resolved lines.

Atmospheric absorption due to water and oxygen present in the laser cavity partly obscures the HDO spectrum in the investigated region. In particular, the A band of molecular oxygen lying between 12900 and 13160 cm^{-1} makes difficult the recording of the HDO spectrum in this region. It was then necessary to drastically reduce the contribution of the intracavity air by placing the Ti:Sa laser in a box where dry nitrogen was continuously flown. After a few minutes, atmospheric absorption was decreased by about two orders of magnitude. The residual absorption was further efficiently suppressed by filling the cell with deuterated water, recording the spectrum, vacuuming the cell and recording the background spectrum. This procedure has the additional advantage of increasing the signal to noise ratio as the fringes frequently appearing on the spectrum baseline are stable over the time scale of the full operation (about 30 s) and can then be efficiently suppressed.

Each 12 cm^{-1} wide portion of the spectrum was recorded with a 3754 diodes silicon array and calibrated independently using reference line positions. As a rule, the $H_2{}^{16}O$ and HDO reference lines provided in the database attached to Ref. [14] and Refs. [3,6], respectively, were adopted as references except in the 12800–13160 cm^{-1} region where these line lists are too sparse and sometimes not reliable. By chance, this spectral region includes transitions of the oxygen A band which is observed between 12900 and 13160 cm^{-1} as a consequence of the residual intracavity oxygen. The O_2 line positions were then used

for wavenumber calibration purpose. We adopted the wavenumber values as provided by the HITRAN database [15] and applied a constant pressure shift of $-0.009\ cm^{-1}$ as measured in Ref. [16]. The wavenumber calibration of the 12 800–12 900 cm^{-1} region was more problematic: we had to combine some reliable FTS line positions [3,14] with line positions *calculated* from well known energy levels in order to build a sufficient set of reference lines. The lack of precise reference lines may have led to errors up to $0.010\ cm^{-1}$ in some very limited cases but we estimate that the accuracy of the wavenumber calibration is on the order of $0.004\ cm^{-1}$ as will be confirmed below by the uncertainty obtained for the energy levels retrieved from several transitions.

The line positions and relative line intensities were then determined by using an interactive least squares multi-lines fitting program assuming a Voigt profile for each line. Line position, integrated line absorbance, Gaussian and Lorentzian widths of each line and the corresponding baseline (assumed to be a linear function of the wavenumber) were derived from the multiline fitting procedure.

The determination of absolute line intensity values requires the knowledge of the HDO partial pressure and of the absorption path length. As in our experiment, the generation time is controlled, the absorption path length is known but an accurate determination of the HDO concentration is more problematic. Indeed, a drawback of the experimental procedure consisting in successively filling and emptying the cell with deuterated water, is that the H_2O:HDO:D_2O proportion may change from one recording to the next. As a consequence of the rapid proton exchange between the gas phase and water adsorbed on

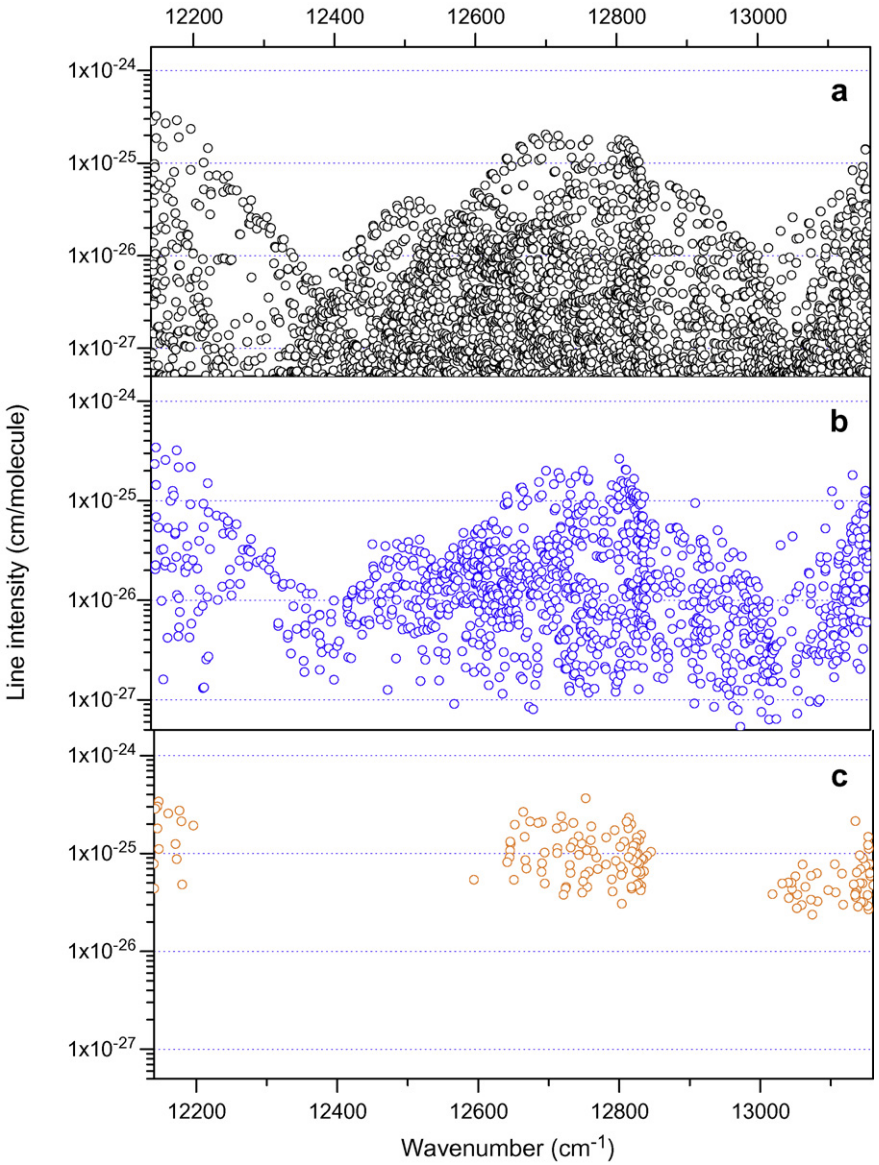

Fig. 2. Overview comparison of the HDO spectrum in the 12 145-13 160 cm^{-1} region. (a) Calculations of Schwenke and Partridge [4,5], (b) ICLAS (this work), (c) FTS spectrum of Refs. [3,6]. Note the logarithmic scale used for the line intensity values. In (a), the SP intensity values were not summed in the case of unresolved multiplets. This is why a few ICLAS intensity values appear to exceed significantly SP values in the case of blended lines.

the wall of the cell, the HDO concentration was observed to evolve with time and consequently from an elementary spectrum to the next one. The situation was even more complicated as the total pressure value itself may decrease during the recording of an individual spectrum, as a result of the adsorption on the cell wall. We then found more consistent and accurate to normalize the relative intensity values retrieved from each elementary spectrum, against the intensity values calculated by Schwenke and Partridge [5]. Such normalization is justified by the good agreement observed up to the visible range between SP intensities and the FTS intensity values of Refs. [3,6].

The most complete line list was obtained by gathering the line lists associated with individual spectra. As several recordings of the same spectral window were often performed and because of overlapping regions, many lines appear several times in this list. The accuracy of the ICLAS line positions being estimated to be around 0.004 cm^{-1}, we considered as identical two lines when both the difference of their positions was less than 0.008 cm^{-1} and their intensities differed by at most a factor of 2. The position and intensities of these identical lines were averaged leading to a global line list which was further checked and cleaned from spurious lines or irreproducible spectral features close to the noise level. The obtained list was then considered for the rovibrational analysis. Fig. 2 illustrates the increased sensitivity compared to previous measurements [3,6] and the good agreement with SP calculations in the overall

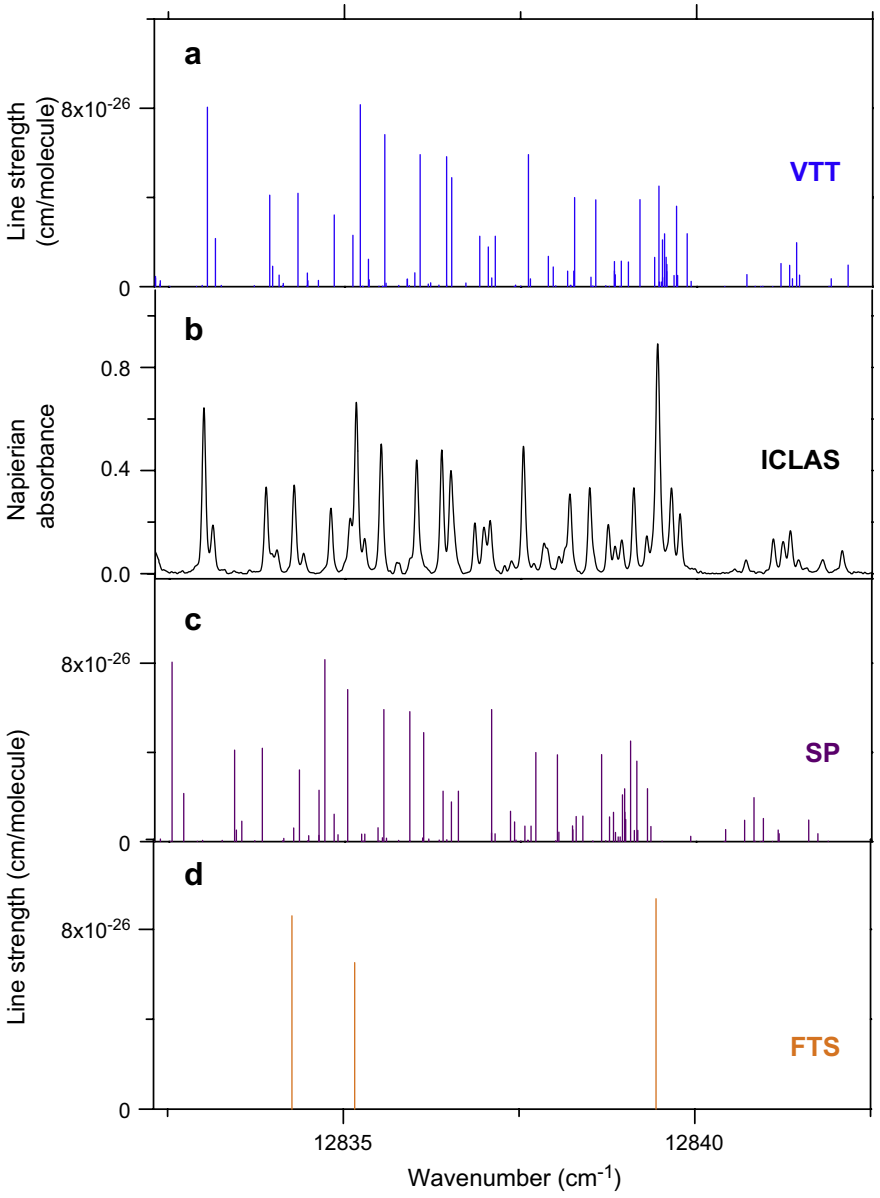

Fig. 3. The spectrum of HDO in the region of the head of the $5\nu_1$ band near 12 840 cm^{-1}: (a) VTT predictions of Refs. [23,24]. (b) ICLAS spectrum of deuterated water recorded at a total pressure of about 18 hPa with an equivalent absorption pathlength of 24 km. In the considered interval, the contribution of H_2O is negligible while D_2O contribution is very limited. (c) Variational calculations of Schwenke and Partridge [4,5], (d) FTS measurement of Refs. [3,6].

region. Similar comparison limited to a small spectral section is presented in Fig. 3.

3. Spectral analysis

3.1. Spectrum assignment and energy levels derivation

The experimental line list contained altogether about 2500 absorption lines which resulted from the H_2O, HDO and D_2O contributions. The H_2O contribution is strong in the low energy part of the studied spectrum and becomes much weaker above 12 700 cm^{-1}. The D_2O absorption lines are relatively strong in the region of the $\Delta v_{OD} = 5$ band around 12 700 cm^{-1} and are observed with weaker intensities up to 13 160 cm^{-1}. The discrimination of the HDO lines was greatly helped by the comparison with the H_2O and D_2O ICLAS spectra that we recorded separately. As reported in Refs. [17,18], we recently obtained a D_2O ICLAS spectrum with enrichment close to 100% while the knowledge of the H_2O spectrum was also improved by our ICLAS measurements in the same region [19,20]. Fig. 4 shows the comparison of the ICLAS spectra in a small spectral section around 12 800 cm^{-1} where the absorption lines of D_2O, HDO and H_2O are on the same order of magnitude. Finally, after identification of the H_2O and D_2O lines, 1185 lines presumably due to HDO were left.

In the most recent HDO studies, the line assignment was based on the comparison with SP predictions [4,5]. These

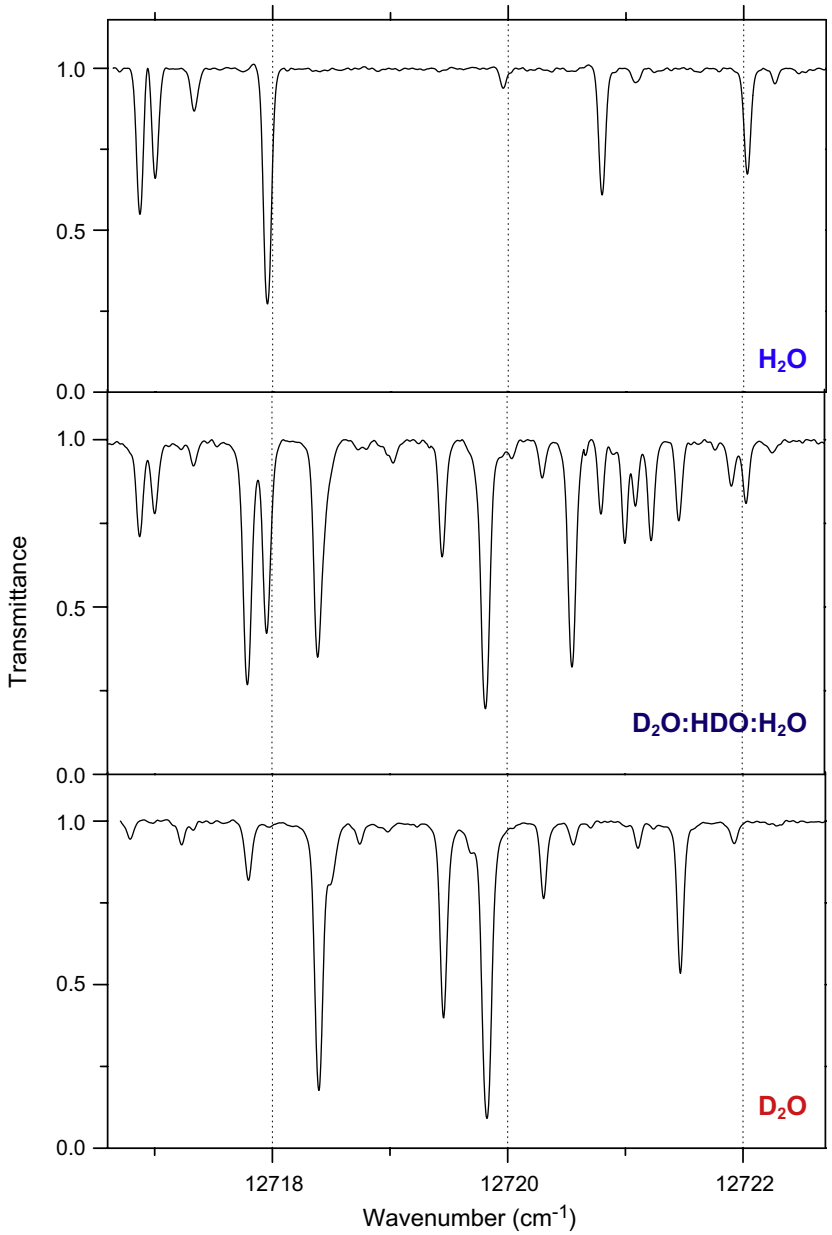

Fig. 4. ICLAS spectrum of H_2O (upper panel), D_2O (lower panel) compared to the ICLAS spectrum of deuterated water (medium panel) showing the superposition of H_2O, HDO and D_2O lines. In the considered spectral interval, transitions of the three water isotopologues have comparable intensities. Such comparison is very useful to discriminate the HDO lines.

calculations were found accurate enough for the assignment of the FTS spectrum of Ref. [3], in the wide spectral range from 11 600 to 26 000 cm^{-1}. However, compared to Ref. [3], our increased sensitivity leads to a much higher density of observed transitions. Compared to the average separation of the weak lines, the accuracy of SP calculations was not sufficient to base our assignments only on the agreement between the observed and calculated line positions. Since the publication of SP results in 1997, many new HDO levels have been determined. A new HDO PES [21] was recently optimized through the fitting to the available HDO energy levels with $J \leqslant 8$. A standard deviation of 0.035 cm^{-1} was obtained for the residuals between the observed and calculated values of 4495 experimental energy levels of more than 90 vibrational states. This PES has been used by some of us with a new, *ab initio* dipole moment surface [22] to compute a comprehensive linelist for HDO, which we refer to as VTT (Voronin, Tolchenov, Tennyson) below. Preliminary results for the VTT linelist have already been given [23] and the full linelist, which is still under construction, will be published elsewhere [24]. As detailed below, a synthetic spectrum obtained from the VTT linelist was used in the assignment process.

As a result of the spectral analysis, 1179 observed HDO lines could be assigned. This number should be compared to the 293 HDO lines detected by FTS in the same spectral region [3,6] (see Fig. 2). Only six lines among the weakest were left unidentified. The line list attached to this paper as Supplementary Material presents the observed HDO wavenumbers followed by the observed and calculated (SP) intensities and rovibrational assignments. As a consequence of double and triple assignments of some lines, it corresponds to 1337 transitions. A number of HDO transitions which are superimposed on the $H_2{}^{16}O$ (25 lines), $H_2{}^{18}O$ (4) or D_2O (51) transitions, as well as lines with tentative assignment are specifically indicated.

Table 1 summarizes the obtained spectroscopic information: 592 rovibrational energy levels belonging to 15 vibrational states were derived, 304 of them being newly determined. New information concerns, mainly, the high J and K_a energy levels of the previously studied (500) state [3,9,10] and three newly observed vibrational states: (202), (122), and (311) at 12 568.190, 12 644.652, and 12 919.938 cm^{-1}, respectively. The newly observed HDO energy levels are listed in Tables 2 and 3 while the complete set is attached to this paper as Supplementary Material. Energy levels derived from blended lines and consequently, with less accuracy, are marked. The tables also include deviations of the experimental values from VTT predictions [24] and the statistical experimental uncertainty for the levels determined from several transitions.

The improved quality of the new HDO VTT linelist is illustrated in Fig. 5, where the (obs. − calc.) deviations of the studied energy levels are plotted versus $J + K_a/J$ for both SP and VTT predictions. The most important VTT and SP deviations are −0.16 and 0.64 cm^{-1}, respectively.

Table 1
Summary of the experimental observations retrieved for HDO from the analysis of the ICLAS spectrum between 12 145 and 13 160 cm^{-1}

$v_1v_2v_3$	Band origins (cm^{-1})			N levels	
	Observed	Calc. (VTT)	Calc. (SP)	Total[a]	New
0 6 1		11 533.35	11 533.48	3	0
1 4 1		11 804.55	11 804.57	3	0
3 3 0	11 958.56[b]	11 958.60	11 958.26	1	0
0 1 3	11 969.7530	11 969.75	11 970.07	84	4
0 10 0		12 164.85	12 165.80	1	1
0 4 2		12 516.42	12 516.63	10	10
2 0 2	12 568.1901	12 568.15	12 568.19	77	77
1 2 2	12 644.6528	12 644.65	12 644.72	72	72
0 7 1		12 694.33	12 694.53	2	2
5 0 0	12 767.1355	12 767.16	12 766.72	120	35
1 8 0		12 852.35	12 852.95	2	2
3 1 1	12 919.9387	12 920.04	12 919.95	76	76
1 5 1		12 986.79	12 986.67	1	1
0 2 3	13 278.3508	13 278.34	13 278.44	77	10
1 0 3	13 331.6061	13 331.59	13 331.74	63	14
Total				592	304

[a] Total number of known energy levels including those available in the literature and those presently determined.
[b] Extrapolated value from Ref [1].

A selected part of the ICLAS spectrum in the region of the head of the $5v_1$ band is shown in Fig. 3 along with the FTS stick spectrum [3,6], VTT and SP predictions. The significant shift of SP line positions with respect to the experimental spectrum is clear, while VTT line centres coincide very well with the observed spectrum. The root mean square value of the differences between observed and VTT energy levels is only 0.05 cm^{-1}. In general, the observed rotational dependence of the (obs. − calc.) deviations is less pronounced for VTT predictions compared to SP data. For instance, in the case of the (500) state, SP deviations range from −0.06 to 0.64 cm^{-1}, while VTT deviations vary from −0.16 to 0.11 cm^{-1}.

Along with the accurate predicted HDO line positions, a reasonable match between the experimental and calculated intensities proved to be a key criterion in the assignment procedure, in particular for the weak lines not included into ground state combination difference (GSCD) relations. Fig. 6 shows the observed-to-SP calculated intensity ratio for the assigned HDO lines. The overall agreement between theory and experiment is quite satisfactory and sufficient to support our line assignments. As only separate SP predicted intensities were used for the scaling of the experimental line intensities, the agreement observed for the whole set of observed lines is then significant.

4. Discussion

The HDO molecule is known to undergo strong centrifugal distortion effects leading to strong high-order resonance interactions involving highly exciting bending states. In this study, a number of transitions reaching high bending states like (151), (061), (071) and (180) were

Table 2
Newly determined rotational energy levels (cm^{-1}) of the (202), (311), and (122) vibrational states of HDO derived from the analysis of the ICLAS spectrum between 12145 and 13160 cm^{-1}

$J\ K_aK_c$	(**202**)				(**311**)				(**122**)			
	E_{obs} (cm^{-1})	$\sigma\times10^3$ cm^{-1}	N	δ (cm^{-1})	E_{obs} (cm^{-1})	$\sigma\times10^3$ cm^{-1}	N	Δ (cm^{-1})	E_{obs} (cm^{-1})	$\sigma\times10^3$ cm^{-1}	N	δ (cm^{-1})
0 0 0	12568.1901	2.0	2	0.04	12919.9387		1	−0.06	12644.6528		1	0.00
1 0 1	12583.0077	2.4	4	0.05	12934.5428		1	−0.06	12659.9464	3.1	2	0.00
1 1 1	12595.8506	1.1	3	0.04	12948.9229	0.2	2	−0.09	12677.0621	2.5	2	−0.04
1 1 0	12598.5967	0.7	3	0.05	D 12951.7969		1	−0.12	12680.3906	1.5	2	0.01
2 0 2	12612.2369	0.8	3	0.04	12963.3961	1.5	2	−0.07	12690.1076	0.2	2	0.00
2 1 2	12622.7513	2.0	4	0.04	12975.3310	1.3	3	−0.10	12704.2910	3.8	2	0.01
2 1 1	12630.9750	2.0	5	0.04	12983.9351	0.6	3	−0.10	12714.1090	0.5	3	0.00
2 2 1	12672.2429	1.2	3	0.02	13031.2220		1	−0.08	12762.6482	3.3	2	−0.01
2 2 0	12673.0263	3.3	2	−0.02	13031.5515	1.5	2	−0.08	12763.1155	1.4	3	0.01
3 0 3	12655.1414	1.1	3	0.04	13005.7875	1.4	2	−0.08	12734.3352	0.2	3	0.00
3 1 3	12662.8609	1.5	5	0.04	13014.7385	2.0	3	−0.08	12744.8514	0.9	2	0.00
3 1 2	12679.2723	2.3	4	0.03	13031.8696		1	−0.08	12764.3940	2.7	3	−0.01
3 2 2	12717.2912	2.9	4	0.02	13075.0112	1.0	2	−0.09	12808.3584	0.1	2	0.00
3 2 1	12719.2630	6.7	5	0.01	13076.5674	1.6	3	−0.07	12810.5342	2.4	2	0.00
3 3 1	12776.9771	1.2	3	0.03	13156.6252		1	−0.10	12898.9974		1	0.01
3 3 0	12777.0059	0.5	3	0.02	13156.6519		1	−0.10	12899.0490		1	0.01
4 0 4	12710.8297	3.6	2	0.03	13060.8852	2.1	2	−0.08	12791.7791	1.3	3	−0.01
4 1 4	12715.9438	0.6	4	0.03	13066.9606	1.9	3	−0.09	12798.5448	0.2	2	−0.01
4 1 3	12743.1276	3.2	3	0.03	13095.2133	0.1	2	−0.10	12830.8873	1.1	2	−0.01
4 2 3	12760.5052	4.8	2	0.01	13133.1102		1	−0.08	12868.9492	1.3	2	0.00
4 2 2	12765.6286	3.4	3	−0.04	13138.4130	1.1	3	−0.04	12875.0051	2.8	2	0.00
4 3 2	12836.6781	2.7	4	0.02	13215.4660	2.7	2	−0.09	12960.8998		1	0.00
4 3 1	12836.9284	2.4	4	0.01	13215.6662	5.0	2	−0.09	12961.3529	3.2	3	0.00
4 4 1	12930.6787	2.7	2	0.02	13327.0122		1	−0.09	D 13090.9187	1.1	2	0.03
4 4 0	12930.6897	7.1	3	0.02	13327.0904		1	−0.08	D 13090.9157		1	0.01
5 0 5	12778.6489	0.6	3	0.02	13127.9275	5.0	2	−0.08	12859.4675		1	−0.02
5 1 5	12781.7620	2.2	4	0.02	13131.7795	1.7	2	−0.09	12863.9743		1	−0.02
5 1 4	12822.0214	0.4	2	0.01	13173.4478	1.2	2	−0.10	12913.3811	2.2	2	−0.05
5 2 4	12834.9714	2.0	3	−0.02	13205.2771	1.7	3	−0.09	12944.1750	1.7	3	−0.01
5 2 3	12846.6999		1	−0.02	13215.9390		1	−0.09	12956.5003		1	−0.04
5 3 3	12911.3984	0.8	3	0.02	13289.1234	2.4	3	−0.10	13038.4121		1	−0.02
5 3 2	12912.3550	0.6	3	0.01	13289.8802	1.7	2	−0.09	13038.4607		1	−0.03
5 4 2	13005.0479	2.2	3	0.01	13400.3993		1	−0.09	13168.8475		1	0.00
5 4 1	13005.0710		1	0.02	13400.2422	3.6	2	−0.09	13169.0314	1.6	3	0.00
5 5 1	13123.4214		1	0.01	13540.2354		1	−0.08	13342.1504		1	0.01
5 5 0	13123.4195		1	0.01	13540.2354		1	−0.08	13342.1504		1	0.01
6 0 6	12858.2958	1.9	4	0.03	13206.4541	0.3	2	−0.09	12940.9773		1	−0.03
6 1 6	12860.0792	0.9	4	0.02	13209.0588	2.7	2	−0.08	12943.8547		1	−0.02
6 1 5	12915.3602		1	0.00	13265.8271	2.5	2	−0.12	13007.3833		1	0.11
6 2 5	12923.2052	1.2	3	0.00	13291.2259		1	−0.10	13033.7925	2.7	2	−0.02
6 2 4	12944.6471		1	−0.02	13310.2093		1	−0.10	13057.6688	2.1	2	−0.02
6 3 4	13001.0514	0.8	3	0.00	13377.5239	2.0	2	−0.11	13131.4794		1	−0.03
6 3 3	13003.7895	2.7	2	0.00	13379.7336	6.6	2	−0.10	13133.5150		1	−0.03
6 4 3	13094.4549		1	0.01	13488.6421		1	−0.09	13262.6932	6.0	2	−0.01
6 4 2	D 13094.5631		1	0.00	13488.5083	6.3	2	−0.10				0.03

6 5 2	D 13212.3256		1	0.02	13627.9306		1	−0.09	D 13435.8980		1	0.01
6 5 1	D 13212.3128		1	0.00	13627.9294		1	−0.09	D 13435.8818		1	
6 6 1	13354.8444		1	0.01								
6 6 0	13354.8444		1	0.01								
7 0 7	12949.7228	1.1	3	0.00	13298.6916	1.7	2	−0.08	13034.3639		1	−0.04
7 1 7	12950.7139	1.4	3	0.00	13296.3146	2.5	3	−0.10	13035.5739	2.5	2	−0.02
7 1 6	D 13022.2065		1	−0.04	13371.4857	0.1	2	−0.11	13117.8370	1.1	3	−0.04
7 2 6	13025.2328	2.6	3	0.00	13390.7219		1	−0.10	13136.1121	1.5	2	−0.04
7 2 5	13057.1011		1	−0.02	13421.0299		1	−0.11	13173.9778		1	−0.02
7 3 5	13105.4838		1	0.00	13481.0961		1	−0.09	13239.9679		1	−0.02
7 3 4					13485.7740		1	−0.12	13245.4900	1.7	2	−0.04
7 4 4	13198.9595	5.1	2	−0.01	13591.7501	5.5	2	−0.13	13372.4241		1	0.01
7 4 3	13199.3912	4.8	2	0.00	13591.7832		1	−0.11	13370.6140	0.4	2	−0.02
7 5 3					T 13730.3507		1	−0.11				
7 5 2					T 13730.3519		1	−0.12	13545.3331	7.2	2	0.00
7 6 2	13458.2027		1	0.00								
7 6 1	13458.2015		1	0.00								
8 0 8	13052.9964	1.2	3	0.00	13400.6352	0.5	2	−0.07	13139.6452	1.6	2	−0.04
8 1 8	13053.5357	3.5	3	0.00	13397.6941	3.9	3	−0.09	13138.8123		1	−0.04
8 1 7					13489.4659		1	−0.11	13240.4397		1	−0.04
8 2 7	13138.1229	1.9	2	−0.03	13503.7508	0.2	2	−0.09	13253.5186	1.9	2	−0.04
8 2 6	13184.9471		1	−0.02	13547.2156		1	−0.10				
8 3 6	13224.4107	2.6	2	−0.01	13598.7292		1	−0.09				
8 3 5	13236.8667		1	0.00	13608.5013		1	−0.12	13375.2048		1	−0.07
8 4 5	13318.6100		1	−0.01					13497.7505		1	−0.04
8 4 4					13710.3215		1	−0.11				
9 0 9	13168.1509	3.4	2	−0.02	13515.7159		1	−0.06	13252.4398	1.5	2	−0.05
9 1 9	13168.4517	6.9	3	−0.01					13254.7201	10.1	2	−0.05
9 1 8	D 13259.1045		1	−0.04	13619.0550		1	−0.11	13374.8166		1	−0.04
9 2 8					13629.8525		1	−0.09	D 13383.5452	4.8	2	−0.04
9 2 7	13326.8329		1	−0.03					13454.6971		1	−0.03
9 3 7	13357.3877		1	−0.03	13730.2059		1	−0.11				
9 3 6	13378.9099		1	−0.05								
9 4 6	13453.3079		1	−0.03	13842.7323		1	−0.12	13639.7909		1	−0.02
10 0 10	13295.1141	5.2	2	−0.09	13631.4918		1	−0.10				
10 1 10	13295.3372	4.8	2	−0.07	D 13635.3844		1	−0.09	13382.5139		1	−0.05
10 1 9					13759.9434		1	−0.12	D 13520.7124		1	−0.07
10 2 9	13403.9385		1	−0.09	13762.0209		1	−0.12				
11 0 11	13434.2157		1	−0.09	T 13770.2200		1	−0.12	13521.9222		1	−0.06
12 0 12									13673.7046		1	−0.07

This list is limited to the *newly* derived energy levels, the complete set of the rotational levels of the considered states being included in the Supplementary Material and compared to previous experimental determinations.

Note. N is the number of lines used for the upper energy level determination and σ denotes the corresponding experimental uncertainty. Δ is the difference between the experimental energy level and the VTT predictions of Refs. [23,24]. *D* denotes the energy level derived from distorted line and then with less accuracy. Energy levels marked with T were derived from lines with tentative assignment (see text).

Table 3
Newly determined rotational energy levels (cm^{-1}) of the (500), (013), (023), (103), (0100), (042), (071), (151) and (180) vibrational states of HDO obtained from the analysis of the ICLAS spectrum between 12145 and 13160 cm^{-1}

$J\ K_aK_c$	E_{obs} (cm^{-1})	$\sigma\times10^3$ cm^{-1}	N	δ (cm^{-1})	$V_1V_2V_3$	$J\ K_aK_c$	E_{obs} (cm^{-1})	$\sigma\times10^3$ cm^{-1}	N	δ (cm^{-1})	$V_1V_2V_3$
6 6 1	13588.5222	1.0	2	0.06	500	9 6 3	D 14535.4965		1	−0.04	023
6 6 0	13588.5222	1.0	2	0.06	500	10 3 8	14289.5816		1	−0.08	023
7 7 1	13871.3978	0.1	2	0.08	500	10 5 5	D 14532.9288		1	−0.12	023
7 7 0	13871.3978	0.1	2	0.08	500	10 6 5	D 14690.8084		1	−0.05	023
8 6 3	13798.0879	2.8	2	0.05	500	10 6 4	D 14690.8427		1	−0.04	023
8 6 2	13798.0858	2.0	2	0.04	500	12 2 11	14463.0318		1	−0.06	023
8 7 2	13982.5299		1	0.08	500	12 2 10	14623.1170		1	−0.10	023
8 7 1	13982.5299		1	0.08	500	14 0 14	T 14640.7594		1	−0.06	023
8 8 1	14193.5972		1	0.11	500	14 1 14	T 14641.1253		1	−0.06	023
8 8 0	14193.5972		1	0.11	500	9 1 8	14036.7278		1	−0.04	103
9 4 6	13639.3917	1.0	3	−0.01	500	9 4 6	14199.5803	0.1	2	−0.02	103
9 5 5	13767.6570	3.0	3	0.03	500	9 4 5	14203.7557		1	−0.03	103
9 5 4	13767.6974	1.9	2	0.01	500	9 5 5	14310.0071		1	−0.02	103
9 6 4	13923.9040		1	0.04	500	10 1 10	14061.2503		1	−0.06	103
9 6 3	13923.9045		1	0.04	500	10 3 7	14293.1075	5.2	2	−0.05	103
10 1 9	13575.2237	0.7	2	−0.08	500	11 2 9	14403.1911		1	−0.07	103
10 2 9	13580.9806	1.7	3	−0.05	500	11 4 8	14519.6024		1	−0.05	103
10 2 8	13642.8743	3.7	2	−0.05	500	12 0 12	14351.9365		1	−0.10	103
10 3 8	13677.2925		1	−0.06	500	12 1 12	14351.9605		1	−0.08	103
10 4 7	13781.2341	2.5	2	−0.01	500	13 0 13	14515.1681		1	−0.09	103
10 4 6	13783.8959	2.0	2	−0.01	500	13 1 13	14515.1563		1	−0.13	103
10 5 6	13908.5192		1	0.01	500	14 0 14	T 14690.3072		1	−0.10	103
10 6 4	14063.7242		1	0.01	500	14 1 14	T 14690.3020		1	−0.12	103
10 7 4	14246.4980		1	0.06	500	2 1 2	12671.4421	3.4	3	−0.07	0 10 0
10 7 3	14246.4953		1	0.06	500	2 2 1	12654.6999		1	−0.02	042
11 1 10	13723.6113		1	−0.05	500	2 2 0	12655.1057		1	0.00	042
11 2 10	13727.1422		1	−0.06	500	3 2 2	12700.2659	0.4	2	−0.02	042
11 3 8	13862.2636		1	−0.05	500	3 2 1	12702.1541	1.8	2	−0.02	042
11 4 7	13942.4414		1	−0.02	500	4 2 3	12777.2276	5.2	2	0.02	042
11 5 7	14063.6071		1	0.00	500	4 2 2	12782.3484	3.1	2	0.00	042
12 5 8	T 14232.9443		1	0.00	500	5 2 4	12851.8994		1	−0.01	042
13 0 13	13913.8368		1	−0.04	500	5 2 3	12866.0878		1	0.01	042
13 1 13	13913.8035		1	−0.12	500	6 2 5	12941.1819		1	−0.02	042
14 0 14	14083.7309		1	−0.09	500	8 1 7	13145.2408		1	−0.03	042
14 1 14	14083.7243		1	−0.11	500	1 1 0	12797.0486	5.8	2	−0.02	071
12 6 6	13666.1107		1	−0.05	013	3 1 3	12860.8112		1	−0.02	071
12 7 5	13831.1393		1	−0.03	013	4 0 4	13136.2154	2.8	2	0.12	151
15 4 11	14120.0524		1	0.00	013	4 1 4	T 13115.1141		1	0.03	180
16 4 13	14279.1081		1	0.00	013	5 1 5	T 13181.6615		1	0.03	180
9 6 4	D 14535.4862		1	−0.04	023						

This list is limited to the *newly* derived energy levels, the complete set of the rotational levels of the considered states being included in the Supplementary Material and compared to previous experimental determinations.

observed as a result of intensity borrowing from strong line-partners. Part of these transitions was observed in our previous study [1], though some are reported for the first time. Transitions involving the (151), (061) and (071) states are strengthened by resonance interaction with the (311), (013), and (500) states, respectively. Two energy levels of the (180) state were derived from very weak experimental lines. In this case, we could not identify the resonance partner from which the intensity borrowing occurred, and the given assignments should be considered as tentative. The most impressive case of high-order interactions provided by this study is the resonance between the (202) 2_{20} level at 12673.026 cm^{-1} and the 2_{12} level at 12671.442 cm^{-1} which is believed to belong to the (0 10 0) state. This 2_{12} level is derived from four transitions, three of them being very weak while the fourth is partly blended by a D_2O line. The inspection of the nodal structure of the corresponding wave function supported our hypothesis that the level in question belongs to highly excited bending state.

As stated in Ref. [3], strong deviations between observed and calculated intensities may result from resonance interactions between rovibrational energy levels. As close resonances are difficult to predict theoretically, they provide a good test on the accuracy of the underlying potential energy surface. The case of the (330)–(000) band is instructive. It was demonstrated [21] that the calculated intensities of the perturbed transitions of this band are determined by the quality of the PES and are not strongly sensitive to the dipole moment surface. The quality of the new HDO PES was examined in relation with the intensities of a number of strongly perturbed transitions involving

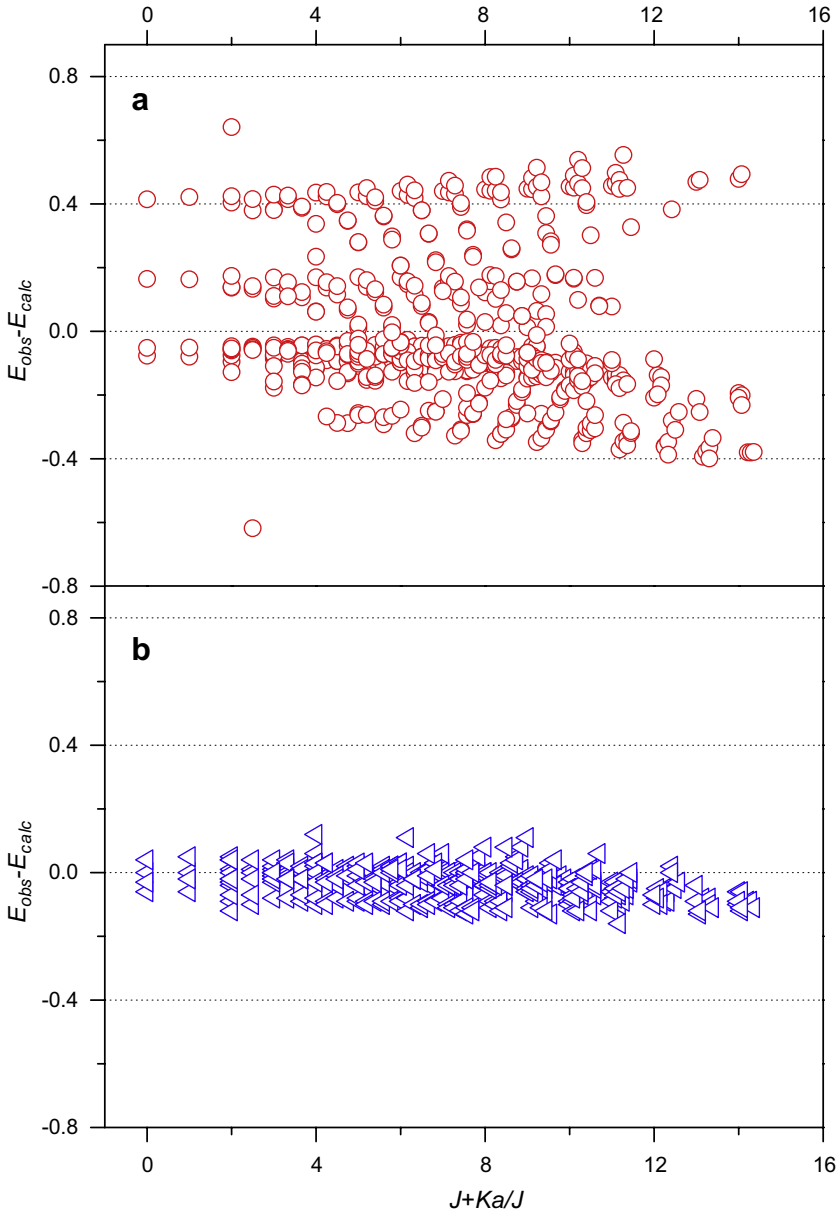

Fig. 5. Differences (in cm^{-1}) between the observed and calculated values for the HDO energy levels determined from the ICLAS spectrum between 12140 and 13160 cm^{-1}. (a) Variational calculations of Schwenke and Partridge [4,5], (b) VTT predictions of Refs. [23,24].

highly excited bending states. Fig. 7 shows the Obs./Calc. ratio for the transitions observed in this work or in our previous study [1], which borrow their intensity from resonance partners. A much better agreement is noted for the VTT calculated intensities while SP intensity values may deviate from the experimental data by as much as a factor 200. A Table placed in the Supplementary Material, lists the considered transitions together with the quantitative comparison of their observed and calculated intensities.

As mentioned above, the whole or parts of the spectral region considered in this study, were previously studied [1,3,7–10]. In the table of the energy levels attached as Supplementary Material, the previous determinations of the energy levels of the (013), (023), (103) and (050) states are included and compared with our values. Good agreement is obtained with the values reported in the recent works [1,3], with *rms* deviation from our values of 0.006 cm^{-1}. Significant deviations with the results of Refs. [7,9] are noted for the (023), (103) and (500) states. A calibration problem was already pointed in Ref. [3]: compared to our values, the (103) and (023) energy levels of Ref. [7] are higher by 0.006 cm^{-1} on average, while the *rms* deviation from our data is 0.013 cm^{-1}. The (500) energy levels of Ref. [9], on the contrary, are underestimated by 0.011 cm^{-1} on average compared to our data with a *rms* deviation of 0.015 cm^{-1}. We also noticed a small negative shift of -0.003 cm^{-1} on average between our values for the (013) state and those of Ref. [8], the *rms* deviation being about 0.011 cm^{-1}.

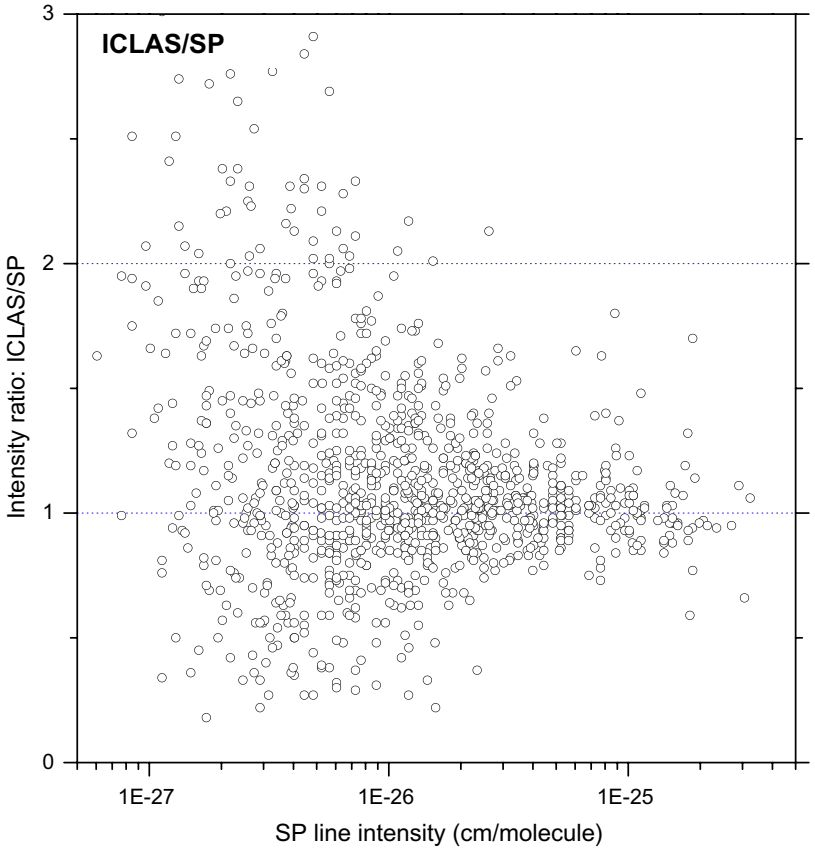

Fig. 6. Ratio of the ICLAS line intensities by the intensity values calculated by Schwenke and Partridge [5]. Note that a number of HDO lines from the resulting linelist was excluded from the comparison in case when they were superimposed to H_2O or D_2O lines.

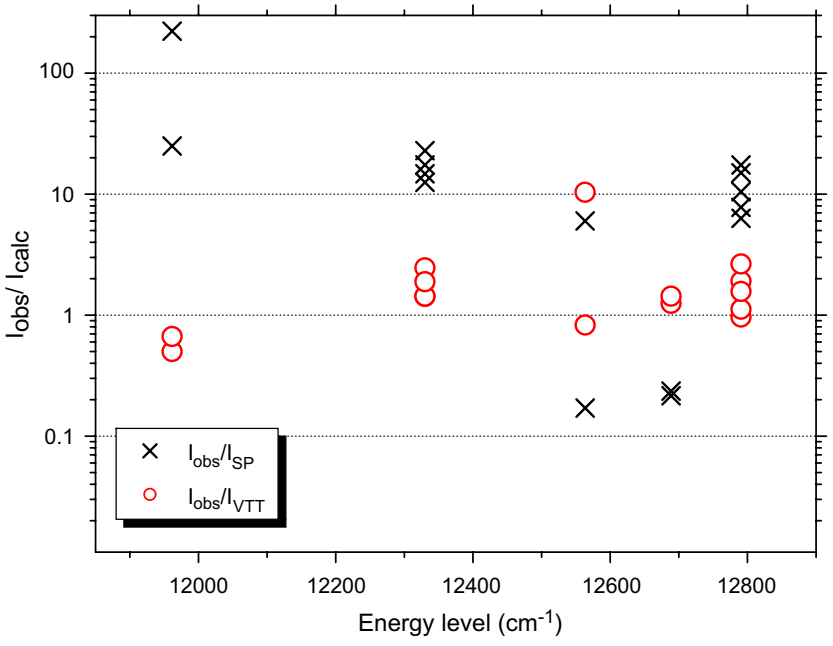

Fig. 7. Variation of the observed to calculated line intensities versus the wavenumber for selected transitions borrowing their intensity from a resonance partner. The considered transitions with their corresponding intensities are listed in a Table provided as Supplementary Material. The ratio values obtained from VTT (Refs. [23,24]) and SP [4,5] calculations are plotted with a different symbol.

The energy levels set for the (500) state was significantly enlarged in this study (120 levels), and we recommend the present set as the most accurate and complete. Compared to our previous studies [1,3,8], only four energy levels were newly determined for the (013) state, the most complete set relative to this state can be found

in Ref. [1] where 179 levels were reported (instead of 84 presently observed).

In the case of the (1 0 3) and (0 2 3) states, 196 energy levels were determined in our previous ICLAS study in the 13 100–13 500 cm^{-1} region [7]. As discussed above, these values are slightly shifted due to a calibration problem. In the present study, 140 energy levels were determined for the (1 0 3) and (0 2 3) set, 24 of them being new. As the center of the $v_1 + 3v_3$ and $2v_2 + 3v_3$ bands are situated well above the investigated region, we observed mostly weak P-branch transitions that resulted in the absence of GSCD and in a certain decrease of accuracy of the energy levels values. The values attached to Ref. [3] (174 energy levels) may be considered as the most accurate for the (1 0 3) and (0 2 3) when supported by GSCD relations; however, energy levels derived in [3] from single weak lines may be equally (sometimes even less) accurate than our present results. Thus, the optimal energy levels set for the (1 0 3) and (0 2 3) states may be obtained by combining the set of Ref. [3] completed with our new observations, with corrected levels from Ref. [7]. We did not attempt to recalibrate our previous data of Ref. [7], as we have recently recorded with a higher sensitivity the HDO spectrum in the 13 160–14 000 cm^{-1} region. The future analysis of this new ICLAS spectrum will improve and replace our previous results [7] and will lead to the most complete dataset for the (1 0 3) and (0 2 3) states.

5. Conclusion

The high resolution rovibrational spectrum of the HDO molecule has been recorded by ICLAS in the wide 12 140–13 160 cm^{-1} region. The assignment of the 1179 HDO lines was performed on the basis of an improved HDO PES [21]. Five hundred and ninety-two accurate energy levels belonging to fifteen vibrational states were derived, 304 of them being newly determined. Transitions reaching the (1 2 2), (2 0 2), and (3 1 1) vibrational states were observed for the first time. The HDO line list provided in the Supplementary Material may be considered as the most complete database in the analyzed region. VTT calculations [23,24] were found to improve significantly SP calculations: (i) on average VTT energy levels values deviate by only 0.05 cm^{-1} from our experimental values, (ii) in the case of strongly perturbed transitions reaching energy levels in strong resonance, the observed line intensities are much better reproduced by VTT calculations than by SP results.

Acknowledgments

This work is supported by a collaborative project between CNRS and RFBR (PICS Grant No. 05-05-22001). This study was performed as part of IUPAC Task Group 2004-035-1-100) to compile, determine, and validate, both experimentally and theoretically, a database of water transitions. A. Campargue is grateful for the financial support provided by the Programme National LEFE (CHAT) of CNRS (INSU). This work was performed as part the QUASAAR Marie Curie Training Network.

Appendix A. Supplementary data

Supplementary data associated with this article can be found, in the online version, at doi:10.1016/j.jms.2007.12.005.

References

[1] A. Campargue, I. Vasilenko, O. Naumenko, J. Mol. Spectrosc. 234 (2005) 216–227.
[2] E. Bertseva, O. Naumenko, A. Campargue, J. Mol. Spectrosc. 221 (2003) 38–46.
[3] B.A. Voronin, O.V. Naumenko, M. Carleer, P.-F. Coheur, S. Fally, A. Jenouvrier, R.N. Tolchenov, A.C. Vandaele, J. Tennyson, J. Mol. Spectrosc. 244 (2007) 87–101.
[4] H. Partridge, D.W. Schwenke, J. Chem. Phys. 106 (1997) 4618–4639.
[5] D.W. Schwenke, H. Partridge, J. Chem. Phys. 113 (2000) 6592–6597.
[6] M. Bach, S. Fally, P.-F. Coheur, M. Carleer, A. Jenouvrier, A.C. Vandaele, J. Mol. Spectrosc. 232 (2005) 329–338.
[7] O. Naumenko, E. Bertseva, A. Campargue, D. Schwenke, J. Mol. Spectrosc. 201 (2000) 297–309.
[8] O. Naumenko, S. –M. Hu, S. –G. He, A. Campargue, Phys. Chem. Chem. Phys. 6 (2004) 910–918.
[9] S. Hu, H. Lin, S. He, J. Cheng, Q. Zhu, Phys. Chem. Chem. Phys. 1 (1999) 3727–3730.
[10] V.V. Lazarev, T.M. Petrova, L.N. Sinitsa, Q.-S. Zhu, J.-X. Han, L.-Y. Hao, Atmos. Oceanic Opt. 11 (1998) 809–812.
[11] A. Campargue, M. Chenevier, F. Stoeckel, Spectrochim. Acta Rev. 13 (1990) 69–88.
[12] A. Kachanov, A. Charvat, F. Stoeckel, J. Opt. Soc. Am. B 11 (1994) 2412–2419.
[13] M. Herman, J. Liévin, J. Vander Auwera, A. Campargue, Adv. Chem. Phys. 108 (1999) 1–431.
[14] R.N. Tolchenov, J. Tennyson, J.W. Brault, A.A.D. Canas, R. Shermaul, J. Mol. Spectrosc. 215 (2002) 269–274.
[15] L.S. Rothman, D. Jacquemart, A. Barbe, D. Chris Benner, M. Birk, L.R. Brown, M.R. Carleer, C. Chackerian Jr., K. Chance, V. Dana, V.M. Devi, J.-M. Flaud, R.R. Gamache, A. Goldman, J.-M. Hartmann, K.W. Jucks, A.G. Maki, J.Y. Mandin, S.T. Massie, J. Orphal, A. Perrin, C.P. Rinsland, M.A.H. Smith, J. Tennyson, R.N. Tolchenov, R.A. Toth, J. Vander Auwera, P. Varanasi, G. Wagner, J. Quant. Spectrosc. Radiat. Transf. 96 (2005) 139–204.
[16] C. Hill, D.A. Newnham, J.M. Brown, J. Mol. Spectrosc. 219 (2003) 65–69.
[17] O.V. Naumenko, F. Mazzotti, O. Leshchishina, J. Tennyson, A. Campargue, J. Mol. Spectrosc. 242 (2007) 1–9.
[18] A. Campargue, F. Mazzotti, S. Béguier, O.L. Polyansky, I. Vasilenko, O.V. Naumenko, J. Mol. Spectrosc. 245 (2007) 89–99.
[19] F. Mazzotti, O.V. Naumenko, S. Kassi, A.D. Bykov, A. Campargue, J. Mol. Spectrosc. 239 (2006) 174–181.
[20] A. Campargue, A.W. Liu, S.N. Mikhailenko, J. Mol. Spectrosc., submitted for publication.
[21] S.N. Yurchenko, B.A. Voronin, R.N. Tolchenov, N. Doss, O.V. Naumenko, W. Thiel, J. Tennyson, J. Chem. Phys., in press.
[22] L. Lodi, R.N. Tolchenov, J. Tennyson, A. E. Lynas-Gray, S.V. Shirin, N.F. Zobov, O.L. Polyansky, A.G. Csaszar, J. van Stralen, L. Visscher, J. Chem. Phys., in press.
[23] J. Tennyson, G.J. Harris, R.J. Barber, S. La Delfa, B.A. Voronin, Y.V. Pavlenko, Mol. Phys. 105 (2007) 701–714.
[24] B.A. Voronin, R.N. Tolchenov, J. Tennyson, submitted for publication.